# Conceptual Design of Short Range - Low Altitude Fixed Wing Unmanned Aerial Vehicle For Landmine Detection

**G. Daisan**
Faculty of Technology, University of Jaffna

## ABSTRACT

Over the past five decades, landmines are creating serious problems all over the world. Even though many UAVs are being developed for demining, many of them are not available to the humanitarian activities. Designing a UAV for demining from the air is challenging and there are only a few UAVs employed in landmines search in Sri Lanka. This research designs a fixed-wing UAV with a total mass of 47 kg, with 10 kg dedicated to payload. It can fly with a maximum speed of 30 m/s continuously for 40 minutes. This UAV detect landmines using ground penetrating radar in no wetted areas. Several manual calculations and software such as Microsoft Excel, XFLR 5, X-Foil, CATIA V5, and ANSYS 19 were used to complete the conceptual design.

**KEYWORDS:** *Demining, fixed-wing UAV, design, Performance*

## NOMENCLATURE

$\frac{W}{S}$ $(N/m^2)$ - Wing loading
$\frac{W}{P}$ $(N/Watt)$ - Power loading
$(L/D)_{max}$ - Maximum lift to drag
$S_{TO}$ $(m)$ – Take off distance
$C_{L_R}$ - Take off rotation lift coefficient
$C_{D_0}$ - Zero-lift drag coefficient
$g$ $(m/s^2)$ - Gravitational acceleration
$\rho$ $(kg/m^3)$ - Density of the air
$C_{Lmax}$ - Maximum lift coefficient
$V_{max}$ $(m/s)$ - Maximum velocity
$V_s$ $(m/s)$ - Stall speed
$\eta_P$ - Propeller efficiency
$V_{TO}$ $(m/s)$ - Take off velocity
$\mu$ - Rolling friction
$\Delta\alpha_{L0}$ $(deg)$ - Change in zero lift angle of attack
$K_E$ - Engine weight factor
$N_E$ - Engine number
$W_E$ $(N)$ - Weight of the engine of the UAV
UAV - Unmanned Aerial Vehicle
CG - Center of gravity
MAG – Mines Advisory Group
GPR – Ground Penetrating Radar

https://doi.org/10.54389/YXKG4947

# 1 INTRODUCTION

Landmines and ammunitions are creating significant threat to the people and animals. After the war in Sri Lanka, the landmines remain in the land and it plays a vital role in civilian's security. Children are at the highest risk since, the unexploded bomb can look like a tempting toy to an inquisitive child (Daisan 2020). Since the end of the war in 2009, MAG has cleared more than 882 square kilometers of land, and demined more than 42,000 mines and 14,800 other unexploded bombs in Sri Lanka (Annual Progress Report on National Mine Action Programme 2013). As indicated by Mine Kafon (Hassani, 2011), a Dutch organization evaluated the required time for complete demining of landmines and other explosives utilizing current strategies to be roughly 1000 years. So building up the quickest demining framework is fundamental, and can be conceivable via an airborne demining framework. The landmines can be found everywhere, including forest, desert, sea shore, buildings and so on (Habib, 2007). Since the UAVs are able to fly through narrow trajectories, close to the ground, move faster and perform difficult maneuver, it is widely employed in demining operations across the world by developed countries. Yet this demining process using drones is not widely employed in Sri Lanka and other developing countries (Gerard-Pearse 2018) due to its high cost of production, operation and maintenance. But serious threats like landmines to human lives have to be removed at any cost since many landmines stay in the ground without degrading for decades. So, designing UAVs are important and will ease the demining process.

Since there are many issues yet to be solved on UAV research and its applications, this research area is going to be expanding in the forthcoming years (Francesco Nex 1, 2019). The requirements for demining UAVs to fly at lower altitudes due to GPR sensor limitations necessitates the development of a low-cost air-based vehicle (Goad and Schorer 2008) (Hassani, 2011). Even though certain demining groups are already employing UAVs for monitoring and mapping purposes, the use of drones in the demining industry in Sri Lanka is not well established.

This paper highlights the importance of designing an affordable yet robust fixed wing UAV with GPR sensor for developing countries. The purpose of this project is to design a fixed wing UAV with a landmine searching sensor with a mass of 10 kg. The steps involved in this project for designing the UAV is followed by various stages and methods such as preliminary design, aerodynamic calculation, propulsion system selection, selection of materials and structural calculations and finally weight calculation and performance analysis. The design process starts with mission requirements and mission profile. The mission profile consists of several stages such as take-off, climbing, cruising, loitering, descending and landing.

# 2 MISSION SPECIFICATION

## 2.1 Mission requirements

Maximum speed: 30 m/s.
Absolute ceiling: not more than 250 m.
Rate of climb: 1.5 m/s maximum
Take-off run: 150 m.
g limit: more than +7.5.
To be able to carry a variety of sensors with a mass of 10 kg
Stall speed: 21 m/s.
Endurance: 40 minutes.
Range: 15 kms.

## 2.2 Mission Profile

The mission profile contains five phases: take-off, climb, cruise, loiter and landing. The UAV is designed to search landmines for 40 minutes. The 15 km range is dedicated to complete all the other four phases.

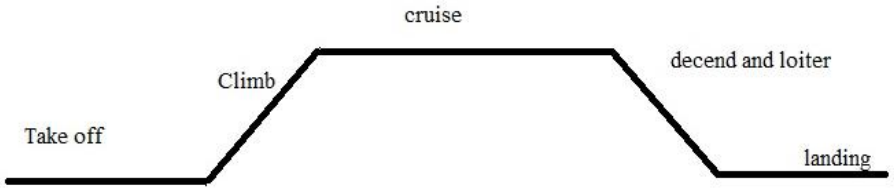


Figure 1. Mission profile

## 3 METHODOLOGY

The camera-ready paper has to be submitted electronically via the website of the conference (http://www.sliit.lk/sices) where a link to the Conference Management System would be found. Please also refer to the website for deadlines.

The UAV design can be divided into four major steps such as conceptual design, preliminary design, detail design, and test & evaluation (Sadraey 2013). In the conceptual design stage of a propeller-driven UAV, the maximum takeoff weight (MTOW) estimation, constraints analysis and conceptual sketch were carried out. From Raymer (Raymer 2018) using equation 1, the MTOW is estimated. To determine the required wing area and power, equations 2, 3, 4 and 5 are used. Conceptual sketch is modelled in CATIA V5.

Maximum takeoff weight (MTOW) estimation:

$$W_{TO} = \frac{W_{PL}}{1-\left(\frac{W_F}{W_{TO}}\right)-\left(\frac{W_E}{W_{TO}}\right)} \tag{1}$$

Wing loading:

$$\left(\frac{W}{S}\right)_{V_s} = \frac{1}{2}\rho V_s^2 C_{Lmax} \tag{2}$$

Takeoff Run:

$$\left(\frac{W}{P}\right)_{S_{TO}} = \frac{1-exp\left(0.6\rho g C_{D_G} S_{TO}\frac{1}{\frac{W}{S}}\right)}{\mu-\left(\mu+\frac{C_{D_G}}{C_{L_R}}\right)\left[exp\left(0.6\rho g C_{D_G} S_{TO}\frac{1}{\frac{W}{S}}\right)\right]}\frac{\eta_P}{V_{TO}} \tag{3}$$

Rate of climb:

$$\left(\frac{W}{P}\right)_{ROC} = \frac{1}{\frac{ROC}{\eta_P}+\sqrt{\frac{2}{\rho\sqrt{\frac{3C_{D_0}}{K}}}\left(\frac{W}{S}\right)}\quad\left(\frac{1.155}{(L/D)max\,\eta_P}\right)} \tag{4}$$

Maximum velocity:

$$\left(\frac{W}{P_{SL}}\right)_{Vmax} = \frac{\eta_P}{0.5\rho_0 V_{max}^3 C_{D_0}\frac{1}{\frac{W}{S}}+\frac{2K}{\rho\sigma V_{max}}\left(\frac{W}{S}\right)} \tag{5}$$

In the preliminary design, wing, horizontal tail, vertical tail, engine, propeller, fuselage, landing gear are sized using following methods. The wing design is followed by several steps such as airfoil selection, calculation of wing parameters and selection of high lift device.

The aspect ratio of the wing is selected from the range based on the conceptual sketch and statistics (Raymer 2018). In order to avoid complexities in wing manufacturing, the simple rectangular shape is selected without twist and dihedral. The stall speed is selected from the mission requirements. The maximum coefficient of lift at stall speed is determined from Sadreay (Sadraey 2013). The suitable airfoil shape is selected from (Eppler, 1990). After selecting an airfoil, the wing analysis is carried out using VLM method (NASA-SP-405, 1976) to verify whether the wing alone produce required coefficient of lift value. Since the airfoil is not producing sufficient lift coefficient, the suitable flap and flap parameters are determined using analytical solution given in Sadraey (Sadraey 2013). The lift increment due to flap deflection is calculated using XFLR (XFLR5, 2019) and NASA TN3911 (Laitone 1989).

$$\Delta\alpha_{L0} \approx -1.15\frac{C_f}{C}\delta_f \tag{6}$$

$$\Delta\alpha_{Lo} = \frac{\partial\alpha}{\partial\delta}\, cos\Lambda_{HL}\delta[1-(a+b\beta)|\delta|] \quad (7)$$

The next component is tail, which includes horizontal and vertical tail. From (Raymer 2018), the tail volume ratio for both tail are determined. And the tail location is determined based on equation 8.

$$l = K_c\sqrt{\frac{4CSV_H}{\pi D_f}} \quad (8)$$

If the tail section is rectangle then dihedral, twist angle, taper ratio and sweep angle should be zero. Since the horizontal tail influences the longitudinal stability, the moment should be balanced. From (Sadraey 2013), the required horizontal lift coefficient is calculated using trim equation 9.

$$C_{L_h} = \frac{C_{m_{owf}} + C_{L\_w}(h-h_o)}{V_H} \quad (9)$$

The airfoil is selected for horizontal tail using equation 9. The tail setting angle is decided based on the trim requirement after calculating the downwash effect due to wing and the longitudinal stability is calculated using equation 10.

$$C_{m_\alpha} = C_{L_{\alpha wf}}(h-h_o) - C_{L_{\alpha h}}\eta_h\frac{S_h}{S}\left(\frac{l}{C}-h\right)\left(1-\frac{d\varepsilon}{d\alpha}\right) \quad (10)$$

For single propeller aircraft, the yawing moment is trimmed by setting the vertical tail at some incidence angle. The initial seizing parameters such as tail volume ratio, aspect ratio and maximum thickness to chord ratio are determined based on the historical data and analytical calculations from Raymer (Raymer 2018).

The engine is selected based on power requirement and is calculated by constraints analysis. The maximum propeller diameter is determined using equation 11.

$$D_P = K_{nP}\sqrt{\frac{2\,P\eta_P AR_P}{\rho V_{av}^2 C_{LP} V_C}} \quad (11)$$

The thrust generated is calculated using momentum disk theory and propeller performance parameters are calculated using analytical approach. After finding these parameters, the suitable propeller is chosen from the manufacturer (Mejzlik, 1974).

One of the crucial components of the aircraft is fuselage. The internal arrangements are carried out based on few parameters and rules such as shape of the fuselage, symmetry, position of fuel tank, payload and other components. The fuselage length to diameter ratio is determined based on historical data available at Sadreay (Sadraey 2013). The shape is determined based on the drag coefficient.

The initial sizing parameters of the landing gear such as height, wheelbase, and wheel track are calculated using analytical approach according to Sadreay (Sadraey 2013). The ground controllability and stability are determined by the analytical method given in Sadreay (Sadraey 2013). The CG of the UAV influences significantly on the position of the landing gear, and the position of front and rear wheel are determined based on tip back and tip forward requirements.

The weights of the components of the aircraft are estimated using the equations 12, 13, 14, 15, 16 and 17. These are based on the statistical methods and empirical relations (Roskam 2018) (Torenbeek, 1982)

### 3.1 Wing Weight

$$W_W = S_W\, MAC\, \left(\frac{t}{C}\right)_{max}\rho_{mat}K_\rho\left(\frac{AR\, n_{ult}}{\cos(\Lambda_{0.25})}\right)^{0.6}\lambda^{0.04}\, g \quad (12)$$

MAC is the Mean Aerodynamic Chord of the wing and taper ratio is $\lambda$. $n_{ult}$ is the ultimate load factor. Sweep angle at the quarter chord position is $\Lambda_{0.25}$. For safety purpose of the aircraft structure, the ultimate load factor is taken as 1.5 times higher than the maximum load factor (Sadraey 2013).

### 3.2 Horizontal Tail Weight

$$W_{HT} = S_{HT}\, MAC_{HT}\left(\frac{t}{C}\right)_{\max HT}\rho_{mat}K_{\rho\, HT}\left(\frac{AR_{HT}}{\cos(\Lambda_{0.25\,HT})}\right)^{0.6}\lambda_{HT}^{0.04}\;\overline{V}_H^{0.3}\;\left(\frac{C_e}{C_T}\right)^{0.4} g \quad (13)$$

$S_{HT}$ is the horizontal tail area, $\left(\frac{C_e}{C_T}\right)$ is the ratio of the elevator to tail chord and $V_H$ denotes the horizontal tail volume ratio.

### 3.3 Vertical Tail Weight

The weight of the vertical tail depends on various parameters such as vertical tail area ($S_{VT}$), material density ($\rho_{mat}$), tail volume ratio, maximum thickness to chord ratio $\left(\frac{t}{C}\right)_{\max VT}$. Empirical equation 14 can be used to calculate the weight of the vertical tail.

$$W_{VT} = S_{VT}\, MAC_{VT}\, \left(\frac{t}{C}\right)_{\max VT} \rho_{mat} K_{\rho\, VT} \left(\frac{AR_{VT}}{\cos(\Lambda_{0.25\, VT})}\right)^{0.6} \lambda_{VT}^{0.04}\ \overline{V}_V^{0.3}\ \left(\frac{C_r}{C_V}\right)^{0.4} g \quad (14)$$

### 3.4 Weight of the Fuselage

$$W_F = L_F\, D_{f_{max}}^2 \rho_{mat} K_{\rho f} n_{ult}^{0.25} K_{inlet}\, g \quad (15)$$

The $K_{inlet}$ is 1 for the aircrafts except for the one which has inlet on the fuselage. So in my case, it is 1. The UAV has a lighter fuselage as it does not carry humans.

### 3.5 Weight of the Landing gear

The height of the landing gear, configuration, material, landing run, speed during the landing, weight at landing and ultimate load factor during the landing are parameters that determine the weight of the landing gear.

$$W_{LG} = K_L\, K_{ret}\, K_{LG}\, W_L\, \left(\frac{H_{LG}}{b}\right) n_{ult_{land}}^{0.2} \quad (16)$$

### 3.6 Weight of the Installed Engine

The required components or installation parts for engine mounting weight is calculated using the empirical relation 17.

$$W_{E\,ins} = K_E\, N_E\, (W_E)^{0.9} \quad (17)$$

Where $K_E\ and\ N_E$ (engine weight factor and engine number) are 3 and 1 respectively.

In the aircraft weight distribution, two parameters are calculated and they are CG and moment of inertia. CG limit is determined using Excel solver option for varying location of the fuel, sensor and systems.

The maneuver diagram is determined based on (Glīzde 2017). The power requirement ($P_{req}$) curve is constructed using equation number 18.

$$P_{req} = \frac{1}{2}\rho V^3 S C_{D_0} + \frac{\frac{W^2}{1/2\rho VS}}{\pi ARe} \quad (18)$$

## 4 CALCULATIONS

Conclusions should state concisely the most important propositions of the paper as well as the author's views of the practical implications of the results.

According to equation 1, the maximum take-off weight is calculated as follows,

$$W_{TO} = \frac{W_{PL}}{1 - \left(\frac{W_F}{W_{TO}}\right) - \left(\frac{W_E}{W_{TO}}\right)} = 461\ N$$

The increment in zero lift angle due to flap deflection is calculated according to equations 6 and 7.

$$\Delta\alpha_0 \approx -1.15 \frac{C_f}{C} \delta_f = -7\ deg$$

$$\Delta\alpha_{Lo} = \frac{\partial\alpha}{\partial\delta}\ cos\Lambda_{HL}\delta[1 - (a + b\beta)|\delta|] = -6.83$$

The location of the tail from CG is determined based on equation 8,

$$l = K_c \sqrt{\frac{4CSV_H}{\pi D_f}} = 1.2\ m$$

The required horizontal lift coefficient is calculated using trim equation 9,

$$C_{L_h} = \frac{C_{m_{owf}} + C_{L\_w}(h - h_o)}{V_H} = -0.1263$$

The longitudinal stability is calculated using equation 10

$$C_{m_\alpha} = C_{L_{\alpha wf}}(h - h_o) - C_{L_{\alpha h}}\eta_h \frac{S_h}{S}\left(\frac{l}{C} - h\right)\left(1 - \frac{d\varepsilon}{d\alpha}\right) = -1.4 \quad 1/rad$$

The maximum propeller diameter is determined using equation 11.

$$D_P = K_{nP}\sqrt{\frac{2\,P\eta_P AR_P}{\rho V_{av}^2 C_{LP} V_C}} = 0.67\ m$$

The wing component weight is calculated from equation 12. Since the wing is rectangular in shape, the sweep angle, taper ratio, and dihedral angle became zero.

$$W_W = S_W\, MAC\, \left(\frac{t}{C}\right)_{max} \rho_{mat} K_\rho \left(\frac{AR\, n_{ult}}{\cos(\Lambda_{0.25})}\right)^{0.6} \lambda^{0.04}\, g = 62.23\ N$$

The horizontal component of the weight of the tail is calculated from equation 13. NACA 0009 airfoil is chosen for both horizontal and vertical tails.

$$W_{HT} = S_{HT}\, MAC_{HT} \left(\frac{t}{C}\right)_{\max HT} \rho_{mat} K_{\rho\, HT} \left(\frac{AR_{\,HT}}{\cos(\Lambda_{0.25\,HT})}\right)^{0.6} \lambda_{HT}^{0.04}\ \overline{V}_H^{0.3} \left(\frac{C_e}{C_T}\right)^{0.4} g = 39.2\ N$$

The vertical component of the weight of the tail is calculated from equation 14

$$W_{VT} = S_{VT}\, MAC_{VT} \left(\frac{t}{C}\right)_{\max VT} \rho_{mat} K_{\rho\, VT} \left(\frac{AR_{\,VT}}{\cos(\Lambda_{0.25\,VT})}\right)^{0.6} \lambda_{VT}^{0.04}\ \overline{V}_V^{0.3} \left(\frac{C_r}{C_V}\right)^{0.4} g = 13.46\ N$$

The weight of the fuselage is calculated from equation 15

$$W_F = L_F\, D_{f_{max}}^2 \rho_{mat} K_{\rho f} n_{ult}^{0.25} K_{inlet}\, g = 59.75\ N$$

The weight of the landing gear is calculated from equation 16

$$W_{LG} = K_L\, K_{ret}\, K_{LG}\, W_L \left(\frac{H_{LG}}{b}\right) n_{ult}^{0.2}{}_{land} = 68.3\ N$$

The weight of the components used for the installation of the engine is calculated from equation 17.

$$W_{E\,ins} = K_E\, N_E\, (W_E)^{0.9} = 10.5\ N$$

## 5 RESULTS

In the preliminary design stage of a propeller-driven UAV, initially, the maximum takeoff weight is determined using equation 1, i.e., 47 kg and 10 kg dedicated to payload. The empty and fuel fractions are 0.67 and 0.08 respectively based on the calculations made by equation 1.

The required wing area is 1.2212 sq. m and power is 12.5 HP, calculated from the constraints analysis (Glīzde 2018). Highest power is required for maximum velocity and take-off phase. Using the equations 2, 3, 4 and 5, the power loading versus wing loading plotted in figure 1.

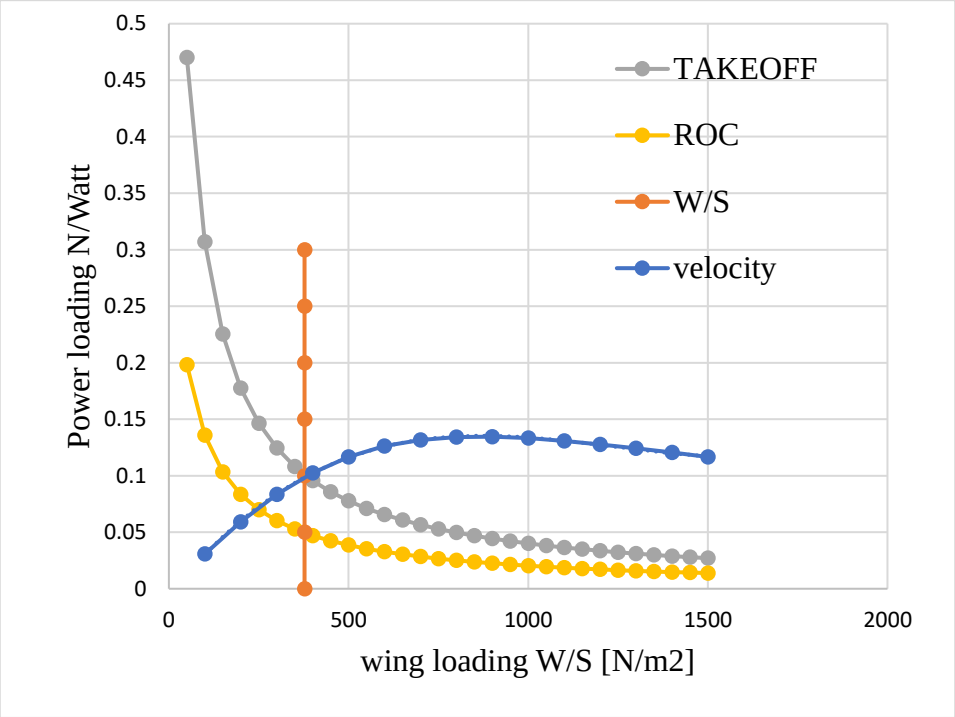


Figure 2. Constraint analysis

The MH 114 airfoil is selected for the wing. The maximum thickness and camber are 13% and 6.4% of the chord length. The maximum thickness and camber are at 28.1% and 50% of chord length respectively. It can be observed from figure 2, the wing lift reduces while comparing it to the airfoil section due to span wise flow and pressure drag. The wing lift coefficient is 30% lower than the airfoil lift coefficient.

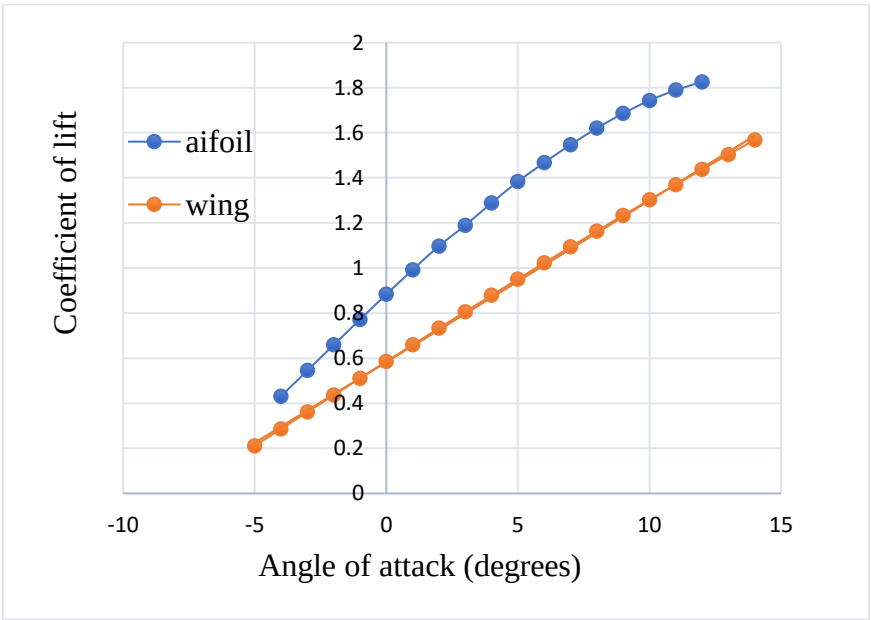


Figure 3. Wing lift and airfoil lift coefficient

The required lift coefficient for the wing at cruise is 0.7141 and it is achieved by setting the wing at 3-degree angle of attack. Since the shape of the wing is rectangle, the taper ratio is 1. The mean aerodynamic chord and the span length are 0.451 m and 2.7 m respectively. Aspect ratio for this rectangular wing is determined by empirical relation given in (Raymer, 2018)

From the historical data, it is decided to dedicate 65 % of the wing span and 30 % of chord to flap. The flap parameters are given in table 1.

Table 1. Flap parameters

| **Type** | **Plain Flap** |
|---|---|
| Flap chord $C_f$ | 0.135 m |
| Flap span$(b_f/2)$ | 0.88 m |
| The required lift coefficient $(\Delta\alpha_{flap})$ | 0.8 |

The zero-lift angle during the take-off is increased when the flap is deflected i.e., camber of the wing increases. The required lift coefficient during the takeoff is around 0.83. When$i_w = 3$, $\alpha_{l=0} = -7.5$ and without flaps, it produces only 0.53 lift coefficient. The required lift coefficient produced after adding flap at 18 degrees was 0.83, and is shown in table 2.

Table 2. Wing lift coefficient with and without flap

| **Characteristics** | **Without Flap** | **With Flap** |
|---|---|---|
| Flap deflection angle | 0 | 18 degrees |
| Wing incidence | $i_w = 3$ | $i_w = 3$ |
| Zero lift angle of attack | $\alpha_{l=0} = -7.5$ | $\alpha_{l=0} = -14.4$ |
| Take off lift coefficient | 0.53 | 0.83 |

The next major component is tail. The vertical and horizontal tails are placed at the rear of the fuselage and both the tails are in the shape of rectangle. The tail volume ratios are 0.5 and 0.04 for horizontal and vertical tails respectively. NACA 0009 airfoil is selected to both tail sections based on horizontal tail lift coefficient. Since both the tails are rectangular in shape, the complexity of manufacturing is reduced. The static longitudinal stability is checked using equation 10, and is found to be -1.4 1/rad. Since the value is negative, the UAV is longitudinally stable.

The total length of the fuselage and wetted area are 2 m and $1.712\ m^2$ respectively. The drag coefficient is 0.07 when the diameter to length ratio is 0.175.

MVVS 116 CC engine is selected in this research work and it has been designed and manufactured by a Czech company called MVVS (Husička, 1953). The maximum power requirement in this project is 12.5 HP which was the initial requirement to search such engine. The thrust required for each phase of the mission is the next essential need. MVVS 116 CC engine could generate up to 14 HP and the technical specification is given in table 3. The maximum diameter of the engine is 300 mm, the maximum width is 122 mm and the length is 275 mm including the shaft which connects the propeller.

Table 3. Technical specifications of the engine

| | | | |
|---|---|---|---|
| Bore | 42 mm | Maximum power output | 14 HP / 6400 RPM |
| Stroke | 42 mm | Maximum Torque | 15 N/m / 6100 RPM |
| Weight of the engine (no ignition system) | 3100 g | Fuel | Unleaded 95- octane |
| Weight of the Ignition system | 270 g | Lubrication | Oil with petrol in mixture 1:40 |

The required propeller diameter is calculated using equation 11 and the performance parameters are given table 4.

Table 4. Propeller performance parameters

| Performance Parameter | Value |
|---|---|
| Thrust | 193 N |
| Propulsive efficiency | 0.84 |
| Thrust coefficient | 0.31 |
| Power coefficient | 0.036 |
| Torque coefficient | 0.058 |
| Advanced ratio | 0.46 |
| Mach number of the tip blade speed | 0.62 |

According to the performance values in table 4, the suitable propeller is chosen.

The height of the landing gear is 0.47 m. The nose gear carries 20 % of the total load of the UAV (154 N) and the main gears carries around 80 % of the total load of the UAV (458 N). The wheel track requirements such as structural integrity, ground stability and controllability for the overturning angle ($\Phi_{ot} \geq 25^{o}$) are 6m, 0.3 m and 63 degrees respectively. These values may change based on further analysis in the subsequent design phases like preliminary and detailed designs.

The weights of the wing, horizontal tail, vertical tail, fuselage, landing gear and engine installation are 62.2 N, 39.2 N, 14 N, 59 N, 68 N and 11 N respectively, and calculated using equations 12, 13, 14, 15, 16 and 17. The calculated CG location after placing the internal components is 1.12 m from the nose, which is not the same as we calculated in the wing and tail design. This value of the CG must be brought down to 0.85 m (0.15 MAC) based on the wing and tail design calculation. It can be done using excel solver option by adjusting the location of the sensor, fuel tank and other systems. After using excel solver, the calculated location for the fuel tank, sensor and systems are 0.6 m, 0.75 m and 1m from the nose respectively.

Figure 4 shows the flight envelope structural limitations and possible maneuvers of the aircraft. This system is molded by aerodynamics, structure, propulsion and aircraft dynamics. The edges of this flight system are called flight envelope or maneuvering envelope.

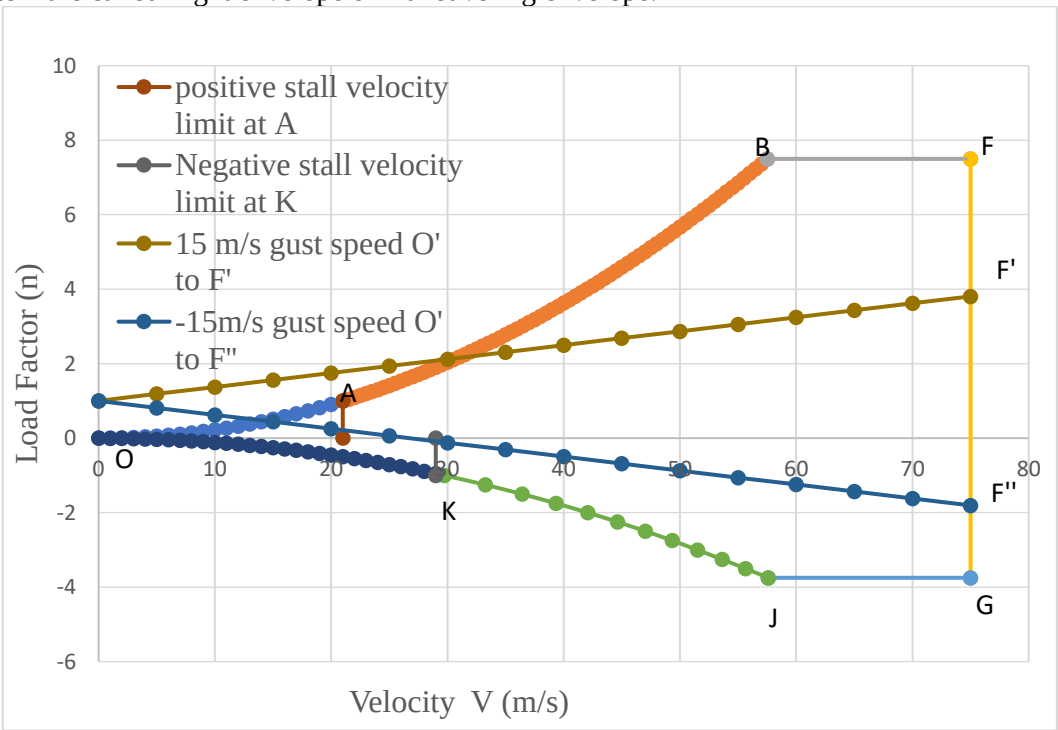


Figure 4. V-n diagram

The negative and positive stall limits, corner load factors and maximum speed limits are calculated based on Glīzde, N. (2017) and is shown in Fig. 4. The maximum positive and negative load factor are 7.5 (point B) and -3.5 (point J) respectively. The gravitational force is one when the aircraft is at cruise condition. The alleviation factor of the gust and gust speed are 0.7 and 15 m/s respectively at cruising at sea level.

The power required versus velocity curve at sea level and 1000 m altitude are constructed using equation 18, and is shown in figure 5.

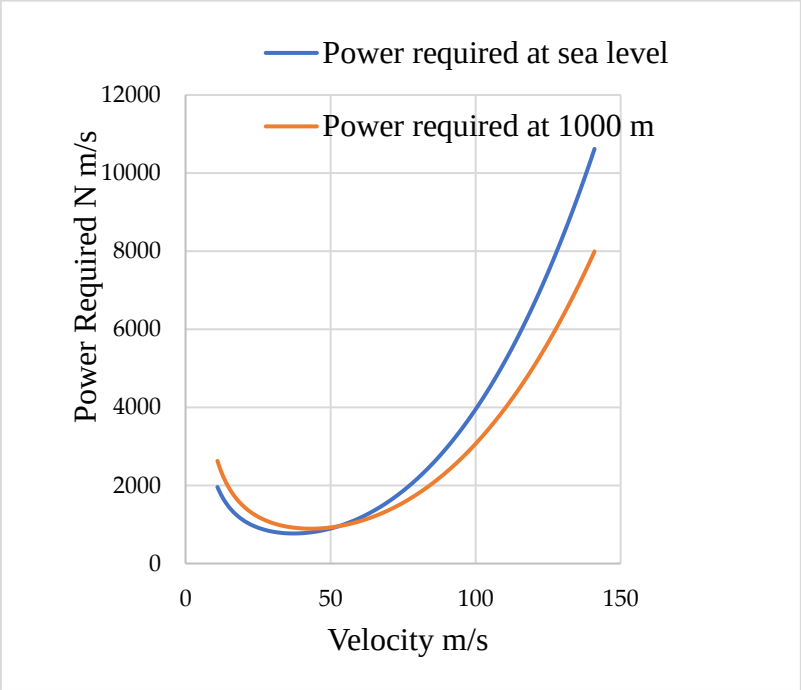


Figure 5. Power required curves

Since the density is lower at 1000 m compared to sea level, the minimum power required at sea level is lower than the power requirement at an altitude of 1000 m. The isometric view of the UAV is given in figure 6 and all the dimensions are in millimeters.

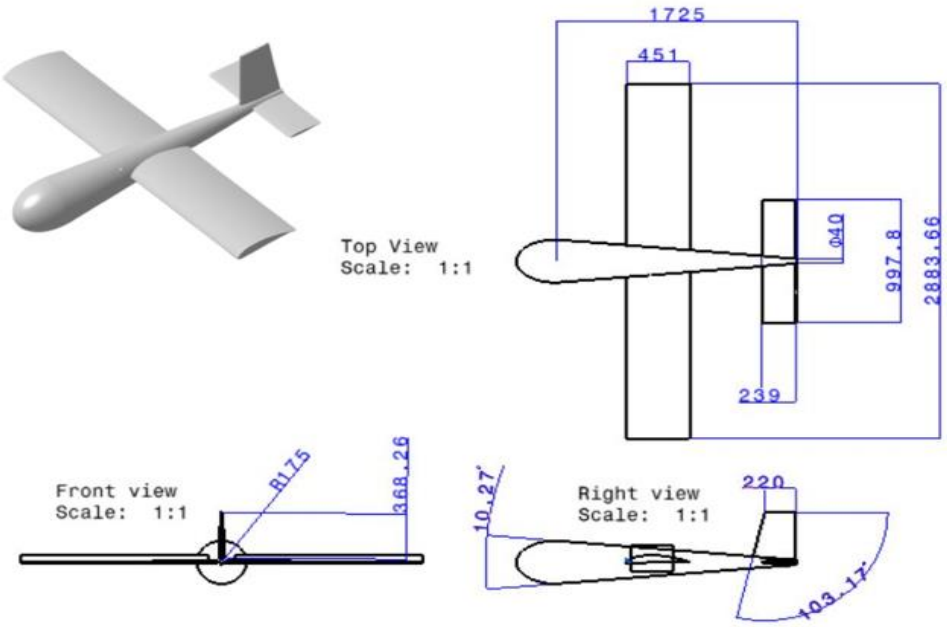


Figure 6. Isometric view

.

## 6 CONCLUSION

A fixed wing was designed to not only for searching landmines but also for humanitarian activities. The conceptual design of the fixed wing UAV is designed with traditional and sophisticated approaches. In this research, a 47 kg weighed UAV is designed with 10 kg dedicated to payload. It can fly with a maximum speed of 30 m/s for 40 minutes; hence the mission specification is achieved. The design started with constraints analysis and followed by sizing of major components & control surfaces, flight envelope and performance calculation. The ANSYS 19 and XFLR software were used for analysis of the components. The future work will focus on optimizing the shape and converting it into a fuel cell-based propulsion system.

## REFERENCES

Annual Progress Report on National Mine Action Programme. (2013). *De-Mining Status-Northern and Eastern Provincess -As at 15 July 2013.Pdf*. http://www.slnmac.gov.lk/publications/annual-progress-reports.html.

Daisan, Gopalasingam. (2020). "Conceptual and Preliminary Design of the Landmine Searching UAS." Warsaw University of Technology. https://repo.pw.edu.pl/info/master/WUT504802048107490f87b4616d62064a1e/.

Gerard-Pearse, Oliver. (2018). "Drones Supporting Mine Clearance in Northern Sri Lanka." *Journal of Conventional Weapons Destruction* 22(3). https://commons.lib.jmu.edu/cisr-journal/vol22/iss3/6.

Glīzde, Nikolajs. (2017). "Plotting the Flight Envelope of an Unmanned Aircraft System Air Vehicle." *Transport and Aerospace Engineering* 4(1): 80–87.

Glīzde, Nikolajs. (2018). "Wing and Engine Sizing by Using the Matching Plot Technique." *Transport and Aerospace Engineering* 5(1): 48–59.

Goad, Aaron, and Daniel Schorer. (2008). "Landmine Detection Utilizing an Unmanned Aerial Vehicle." In *Proceedings of the 2008 IEEE Systems and Information Engineering Design Symposium, SIEDS 2008*, , 231–36.

Laitone, E. V. (1989). "Lift-Curve Slope for Finite-Aspect-Ratio Wings." *Journal of Aircraft* 26(8): 789–90.

Raymer, Daniel. (2018). "Aircraft Design: A Conceptual Approach, Sixth Edition." *Aircraft Design: A Conceptual Approach, Sixth Edition*.

Roskam, Jan. 2018. *Airplane Design*. DARcorporation.

Sadraey, Mohammad H. (2013). John Wiley & Sons, Ltd *AIRCRAFT DESIGN A Systems Engineering Approach*.

Eppler, R. (1990). *Airfoil Design and Data* (1 ed.). Stuttgart: Springer, Berlin, Heidelberg. doi:https://doi.org/10.1007/978-3-662-02646-5

Francesco Nex 1, F. R. (2019, 03 14). Preface: Latest Developments, Methodologies, and Applications Based on UAV Platforms. *MDPI*, 03.

Habib, M. K. (2007). Humanitarian Demining: Reality and the Challenge of Technology – The State of the Arts. *International Journal of Advanced Robotic System, 4*(2), 151-172. doi:https://doi.org/10.5772/5699

Hassani, M. a. (2011). *minekafon.org*. https://minekafon.org/

Husička, Z. (1953). *https://www.mvvs.cz/en/uav-engines*. www.mvvs.cz: https://www.mvvs.cz/en/

Mejzlik, T. (1974). *www.mejzlik.eu*.

NASA-SP-405. (1976). *Vortex-Lattice Utilization.* Virginia: NATIONAL AERONAUTICS AND SPACE ADMINISTRATION.

Torenbeek, E. (1982). *Synthesis of Subsonic Airplane Design* (First ed.). Delft: Delft University Press. doi:https://doi.org/10.1007/978-94-017-3202-4

XFLR5. (2019). *http://www.xflr5.tech/xflr5.htm*.